Molecular BioSystems

Accepted Manuscript

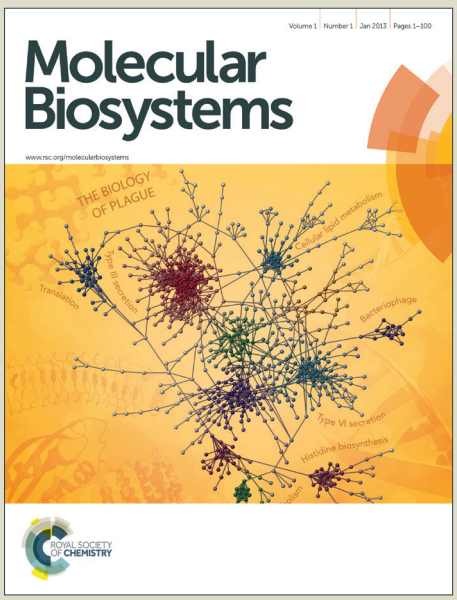

ROYAL SOCIETY OF CHEMISTRY

www.rsc.org/molecularbiosystems

Graphical and textual abstracts for Table of contents entry

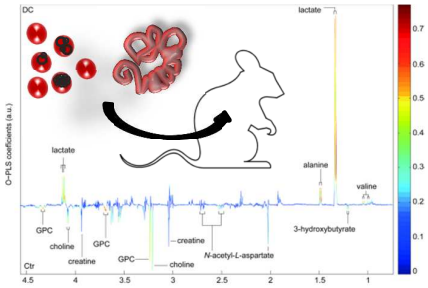

The purpose of this study was to give a comprehensive insight into the systemic metabolic phenotype of mice with a single or dual infection with *Plasmodium berghei* and *Heligmosomoides bakeri*.

Comparing Systems Metabolic Responses in the Mouse to Single or Dual Infection with *Plasmodium berghei* and *Heligmosomoides bakeri*

Lucienne Tritten[1,2,3], Jennifer Keiser[1,2], Tasneem Karwa[4], Jürg Utzinger [2,5], Elaine Holmes[4], Jasmina Saric[4*]

1 Department of Medical Parasitology and Infection Biology, Swiss Tropical and Public Health Institute, Basel, Switzerland, **2** University of Basel, Basel, Switzerland, **3** Institute of Parasitology, McGill University, Sainte-Anne-de-Bellevue, Québec, Canada, **4** Division of Computational and Systems Medicine, Department of Surgery and Cancer, Faculty of Medicine, Imperial College, London, United Kingdom, **5** Department of Epidemiology and Public Health, Swiss Tropical and Public Health Institute, Basel, Switzerland

* E-mail: jasmina.saric@imperial.ac.uk

Abstract

Concomitant infections with *Plasmodium* and gastrointestinal nematodes are frequently observed in humans. At the metabolic level, the cross-talk between host and multiple coexisting pathogens is poorly characterized. The purpose of this study was to give a comprehensive insight into the systemic metabolic phenotype of mice with a single or dual infection with *Plasmodium berghei* and *Heligmosomoides bakeri*. Four groups of eight NMRI female mice were infected with *P. berghei* or with *H. bakeri*, or both species concurrently. An additional group remained uninfected, and served as control. Mice were sacrificed at day 19 of the experiment. We collected samples from liver, spleen, kidney, three intestinal regions, and four brain regions. All biological samples were subjected to ^{1}H nuclear magnetic resonance spectroscopy, combined with multivariate data analysis, to establish metabolic fingerprints from each tissue from the various infection groups. Compared to uninfected mice, single and dual species infection models showed unique metabolic profiles. *P. berghei* exerted major effects on glycolysis, the tricarboxylic acid cycle, nucleotide, and amino acid metabolism in all studied tissues with the exception of the gut. *H. bakeri* was characterized by a dysregulation of choline and lipid metabolism in most tissues examined with a particularly strong imprint in the jejunum. Simultaneous co-infection with *P. berghei* and *H. bakeri* induced the strongest and most diverse effects in the liver and spleen but lead to only minor changes in the intestinal and cerebral parts assessed. Infection with *P. berghei* showed more pronounced and systemic alterations in the mice metabolic profile than *H. bakeri* infection. The metabolic fingerprints in the co-infection models were driven by *P. berghei* infection, whilst the presence of *H. bakeri* in co-infections had little effect. However, simultaneous co-infection showed indeed the least metabolic disruptions in the peripheral tissues, namely gut and brain.

Introduction

Concomitant infections with *Plasmodium* (the causative agent of malaria) and helminths (e.g., the two hookworm species *Ancylostoma duodenale* and *Necator americanus*) are commonly observed in human populations, since they are often endemic in the same warm and humid areas of the world. In sub-Saharan Africa, as many as 25% of school-aged children are considered to be at risk of co-infection with *Plasmodium falciparum* and hookworm.[1] Field studies have shown a positive association between hookworm infection and malaria prevalence, with implications on potential aggravation of clinical outcomes such as anemia.[2, 3] Although attempts have been made to deepen our understanding of alterations in the host metabolism due to single species infections in animal models[4, 5], the interplay between the host and the two pathogens remains poorly characterized. The systemic distribution of the malaria parasite throughout the body may result in a more global effect on the host metabolism; however, localized helminth infections have also been shown to exert remote effects on the metabolic profile of the mammalian host.[6]

Metabolic profiling, which combines spectroscopic profiling of biological samples with multivariate data analysis, has enabled the study of dynamic metabolite expression at various physiological levels over time. This approach, which has adopted predominantly ^{1}H nuclear magnetic resonance (NMR) spectroscopy, has been successful in many different *in vivo* and *in vitro* systems, modeling parasitic infections, and has shed new light on intricate host-parasite interactions. Comparing metabolic data across different rodent-parasite models suggests that each parasite species induces a unique metabolic fingerprint in the rodent host.[7] Indeed, the methodology has facilitated our understanding of the global metabolic effects in rodent models with experimental infections with *Echinostoma caproni*, *Schistosoma mansoni*, *Fasciola hepatica*, and *Plasmodium berghei*.[5, 6, 8, 9] For instance, a study on biofluids from *P. berghei*-infected mice characterized infection-related decreases in plasma glucose and glycerophosphocholine (GPC) concentrations, coupled with increased levels of urinary pipecolic acid, amongst other metabolic disturbances.[5] More recently, the effects of

Plasmodium infection on murine metabolism were further assessed in urine, serum, liver, and brain.[10, 11] Sexual dimorphism was evident in the metabolic response to the infection, indicating that males were less capable of maintenance of serum homeostasis than their female counterparts.[11, 12] In both cerebral and non-cerebral forms of the disease, a general down-regulation of glucose and increase of glutamine/glutamate serum and liver levels was seen, as well as lower levels of choline species in the brain. Hallmarks of cerebral malaria were manifested in perturbed neural lipid metabolism and also affected the ammonia detoxification pathway.[10]

Thus far, fewer data are available on experimental infections with gastrointestinal nematodes. *N. americanus* was shown to perturb energy metabolism and to disrupt the gut microbiota in the hamster, in a study using urine, blood, and worm extracts from infected hamsters.[4] Depleted glucose levels and increased concentrations of lipid metabolites characterized infections with this anemia-causing nematode. Unique to the infection, was the presence of higher amounts of 2-aminoadipate, a metabolite of the kynurenine pathway, in urine when compared to uninfected control animals.[4]

In the present work, we created four different single or co-infection scenarios using the murine malaria parasite *P. berghei* and the rodent gastrointestinal helminth *H. bakeri*, often used as a model of hookworm infections.[13] Findings from urine and plasma collected and analyzed in the framework of the present study have been published elsewhere.[14] In brief, the urinary profile largely overlapped with those obtained by Li and colleagues in the *P. berghei*-mouse model [5], that was characterized by elevated pipecolic acid levels and by the presence of two newly described metabolites, 4-amino-1-[3-hydroxy-5-(hydroxymethyl)-2,3-dihydrofuran-2-yl]pyrimidin-2(1H)-one and 2-amino-4-({[5-(4-amino-2-oxopyrimidin-1(2H)-yl)-4-hydroxy-4,5-dihydrofuran-2-yl] methyl}sulfanyl)butanoic acid.[14] Infection with *P. berghei* drove a stronger metabolic response in plasma compared to *Heligmosomoides bakeri*, indicating malaria caused dysregulation of glycolysis and amino acid metabolism[14], which is in line with findings from Li *et al.*[5]

94 The purpose of this study was to provide a comprehensive map of systemic and
95 localized metabolic dysregulation in mice infected with *P. berghei*, or *H. bakeri,* or both
96 species concurrently. Findings reported here might provide new metabolic insight into the
97 implication of co-infection in human populations.

98

Materials and Methods

Ethics Statement

Experiments were carried out to best comply with the 3R rules (i.e. reduce, replace, and refine) for animal experiments. The present study was approved by the cantonal veterinary office Basel-Stadt and carried out in accordance with the cantonal and Swiss national regulations of laboratory animal welfare (permission no. 2081).

Experimental Set-up

Detailed information on the study design and experimental procedures have been described elsewhere.[14] In brief, 40 NMRI female mice aged three weeks were randomly allocated into five groups of eight animals, and allowed to acclimatize for a week. The five groups are as follows: (i) *P. berghei* single infection (group P); (ii) *H. bakeri* single infection (group H); (iii) delayed co-infection (group CD); (iv) simultaneous co-infection (group CS); and (v) uninfected control (group Ctr). After acclimatization, designated day 0, groups H and CD were administered 80 infective *H. bakeri* third stage larvae (L_3) in 150 µl tap water by oral gavage.[15] On day 15, groups P, CD, and CS were injected 2 x 10^7 erythrocytes, parasitized with a *P. berghei* ANKA strain (GFP-transfected) at a volume of 0.2 ml intravenously.[16] Group CS was co-infected with 80 L_3 *H. bakeri* on day 15. All mice were euthanized by spinal dislocation on day 19. Brain, liver, spleen, right kidney, and sections of colon, ileum, and jejunum were removed from each mouse. The samples were rinsed in PBS, frozen over dry ice and stored at -80 ℃ until shipment to Imperial College London for ^{1}H NMR spectroscopy and multivariate data analysis.

Sample Preparation

The brains were separated into four parts: (i) frontal cortex; (ii) cerebellum; (iii) brain stem; and (iv) remaining brain region prior to tissue extraction. The remaining brain region included midbrain, thalamus, hippocampus, hypothalamus, and the middle regions of the cerebral cortex. From each mouse (eight per group), one sample from each tissue was processed and analyzed individually. Tissues were weighed to ~100 mg (liver, right kidney, spleen, and brain regions) or ~50 mg if the overall volume was smaller (i.e., colon, ileum, and jejunum) and immediately immersed in a tube containing 400 µl ice cold methanol (≥99.9%). For 100 mg tissue, 400 µl methanol 100% (4 ℃, Fluka, Dorset, United Kingdom) were added to 2 ml screw-cap tubes containing 1 g Zirconia beads (Ø 1.0 mm Zirconia beads, BioSpec Products, Bartlesville, United States of America). Subsequently, 285 µl H_2O (Fluka) and 400 µl chloroform (Sigma-Aldrich, Dorset, United Kingdom) were added to 100 mg tissue, or 142.5 µl H_2O and 200 µl chloroform were added to 50 mg tissue. Tissues were homogenized using a bead beater (Precellys 24, Bertin Technologies, Montigny-le-Bretonneux, France) at 6,370 x *g* for 30 s, followed by centrifugation for 10 min at 18,890 x *g* (Sigma 1-14 microcentrifuge, Sigma Centrifuges, Osterode am Harz, Germany). The aqueous phases were carefully transferred into new Eppendorf tubes and dried overnight in a speedvac (Eppendorf, Hamburg, Germany, program: 1-2 x 30 s at 6,370 x *g*). Extracts were dissolved in phosphate buffer (43.8 mM NaH_2PO_4 and ~ 0.2 M Na_2HPO_4, 70% D_2O v/v, 0.1% sodium 3-(trimethylsilyl) propionate-2,2,3,3-d_4, pH=7.4), transferred into NMR tubes (NMR sample tubes, diameter: 4.1 mm, length: 17.78 cm, Wilmad labGlass, Vineland, United States of America), and stored at 4 ℃ prior to data acquisition.

^{1}H NMR Data Acquisition

^{1}H NMR spectra were acquired from each tissue extract on a Bruker 600 DRX MHz spectrometer (Rheinstetten, Germany). A standard 1-dimensional (1D) experiment with a solvent suppression pulse delay [recycle delay (RD)-90°-t_1-90°-t_m-90°-acquire free induction

decay (FID)] was used.[17] A 2 s long relaxation delay (RD) was applied, t_1 was chosen at 3 ms, and mixing time (t_m) set to 100 ms. Water irradiation was achieved during RD and t_m. Spectral width was 20.017 p.p.m. and acquisition time for each sample was set to 2.72 s. A 0.3 Hz line broadening factor was applied to the FID, which underwent Fourier-transformation to obtain spectra of 64 K points resolution. Each sample was scanned 128 times, at a constant temperature of 300 K.

Data Processing and Multivariate Analysis

All ^{1}H NMR spectra were manually phased and baseline-corrected in Topspin (version 3.1, Bruker, Rheinstetten, Germany), and aligned on sodium 3-(trimethylsilyl) [2,2,3,3-$^2H_4$] propionate (TSP) at δ 0.00. The complete spectra were imported into MATLAB (version 7.12.0, R2011a, Matlab, Natick, MA, United States of America). The spectral region containing the water peak (in all spectra) as well as spectral segments containing peaks from ethanol and methanol were removed as follows: (i) liver: 1.15-1.20, 3.32-3.39, 3.64-3.69, 4.55-5.20 p.p.m.; (ii) spleen: 4.70-5.12 p.p.m.; (iii) right kidney: 3.35-3.37, 4.35-4.60 p.p.m.; (iv) colon: 1.15-1.20, 3.31-3.40, 3.64-3.70, 4.55-4.20 p.p.m.; (v) ileum: 3.35-3.37, 4.40-4.45 p.p.m.; (vi) jejunum: 1.17-1.20, 3.35-3.38, 3.64-3.71, 4.54-5.05 p.p.m.; and (vii) brain regions: 4.69-5.50 p.p.m. In addition, median-fold normalization and peak alignment were applied using in-house developed scripts.[18] In order to identify biomarkers that are discriminating infection states, orthogonal projection to latent structure-discriminant analysis (O-PLS-DA) was employed to compare ^{1}H NMR spectral data in pairwise fashion between the different infection groups and the uninfected control mice.[19, 20] O-PLS-DA produces correlation coefficient plots displaying systematic variation between infection groups. The degree of significance can be visualized using the color scale, where red stands for high significance and blue for low significance. The significance cutoff was set at a p-value of 0.05. Back-scaling of the covariance matrix was implemented to keep the initial spectral structure and

enables interpretability of the plots. The O-PLS-DA algorithm includes a 7-fold cross validation. The higher the cross-validation parameters Q^2, the more robust the model. Metabolite identities were determined using in-house databases, statistical total correlation spectroscopy (STOCSY)[20] to link related peaks, the software Chenomx Profiler (Chenomx NMR Suite version 7.1, Chenomx, Edmonton, Canada), as well as published literature for confirmation.

Results

Physiological metrics and analysis of mouse weight, blood packed cell volume (PCV), *P. berghei* parasitemia, and numbers of *H. bakeri* worms upon dissection have been presented elsewhere.[14] In brief, there was no significant difference between the weight of mice and blood PCV when comparing all infection groups in a pairwise manner. Similarly, the presence of the second parasite in the co-infection models did not influence on *P. berghei* parasitemia or *H. bakeri* worm counts, compared to groups harboring a single infection.

The metabolic profiling strategy uncovered infection-related changes in all tissues assessed. Forty-two different metabolites were found changed by any of the pairwise infections group comparisons. Comparing the total number of metabolic dysregulation across the brain, liver, spleen, right kidney, and the intestinal portions, the spleen showed by far the largest amount of biomarkers of infection (n=132) and generated the most robust statistical models based on the Q^2 value (metric of predictive ability of the O-PLS-DA model), which ranged from 0.23 to 0.89 for the spleen but from -0.43 to 0.63 for the intestinal models, whereby values below 0 indicate that there is no statistical difference in the metabolic phenotype of the two groups compared. The brain, liver, and kidney manifested a similar total amount of biomarkers per tissue (n=72, 66, and 60, respectively) and the total intestinal response resulted in 48 significantly altered metabolites. Among the groups compared, it was obvious that *P. berghei* was driving the majority of metabolic disruption, as evidenced when

any of the groups infected with *P. berghei* (P, DC, and SC) were compared to the remaining two groups where *P. berghei* was absent (H and Ctr). The fewest metabolic differences between groups were found in pairwise comparisons of *P. berghei* infection groups, i.e., P *vs.* DC; P *vs.* SC; and DC *vs.* SC. All candidate biomarkers from the pairwise comparisons are summarized in Table S1.

Liver

The liver metabolite profile was characterized by the presence of glucose and branched-chain amino acids (Table S1, Fig. 1: all infections vs. control). A trend for increased glucose levels was observed, for instance, in groups P and DC. Higher glutamate levels were found in most of the *P. berghei* infection groups across comparisons with the *H. bakeri* single infection and the uninfected control group. The same tendency was found with lactate, aspartate, and succinate. Groups P and SC (but not DC) elicited higher hepatic aspartate concentrations than those groups infected solely with *H. bakeri* or the uninfected controls. All *P. berghei*-infected groups displayed lower adenosine and inosine levels compared to group H and Ctr, and higher levels of phosphocholine (PC) when compared to controls. Augmented alanine, leucine, isoleucine, and valine levels were uniquely found in the two co-infected groups, as compared to the *H. bakeri* single infection or uninfected control groups, however, not in each comparison involving a co-infection group. The simultaneous co-infection group displayed lower fumarate levels than all other groups. Greater amounts of lipids represented *H. bakeri* in groups H and SC.

Spleen

The spleen showed a high degree of overlap between metabolic effects due to *P. berghei* and *H. bakeri* infection. While uridine, inosine monophosphate (IMP), and alanine levels were affected by both parasite species, decreased levels of uracil and inosine were found in mice infected with *P. berghei* compared to controls or *H. bakeri* mono-infection. Higher levels of lysine, leucine, isoleucine, valine, tyrosine, and phenoacetylglycine,

aspartate, glutamate, and lactate were discriminatory in all infections with *P. berghei.* However, these perturbations did not always appear consistently in all comparisons with *P. berghei vs*. uninfected groups. GPC levels were decreased by *P. berghei*, especially in co-infection groups, while PC and *scyllo*-inositol were specifically depleted in the simultaneous co-infection model. Reduced levels of *myo*-inositol and betaine were found in mice after infection with *P. berghei*.

Fumarate was consistently and specifically depleted in the spleen of *H. bakeri*-infected mice, compared to the *P. berghei* single infection group and the uninfected control mice. Full details are presented in Table S1 and Fig. 1 (all infections vs. control).

Kidney

The impact of *P. berghei* single and co-infection on the kidney metabolic profile of mice was characterized by increased levels of leucine, valine, phenylalanine, tyrosine, and glutamate (Table S1, Fig. 1: all infections vs. control). Relative concentrations of inosine and IMP were decreased in the *P. berghei*-infected groups. Choline levels were reduced in renal tissue by both parasites and no biomarker was identified that was unique to *H. bakeri* infection.

Gut

Generally, the intestinal tissue presented little infection-related metabolic perturbation (Table S1). Increased tyrosine and inosine were expressed in the colon in the delayed co-infection model, whilst a depletion of 3-hydroxybutyrate and *myo*-inositol were observed in the *P. berghei* single infection model. In the ileum, most metabolic perturbations were observed in the delayed co-infection compared to uninfected controls, as illustrated by an increase in aspartate, choline, and dimethylamine, amongst other metabolites (Fig. 2: all infections vs. control).

Within the jejunum comparison, group DC presented the most significant change as compared to all other groups. Increased levels in GPC were found to be specific to the *H. bakeri* infection, across single and co-infection with *P. berghei*. Moreover, succinate and PC were increased in groups H and CD, although not systematically in all comparisons. The only specific metabolic dysregulation attributed to *P. berghei* infection in the jejunal tissue was a depletion of 3-hydroxybutyrate, when compared to controls.

Brain

None of the comparisons involving frontal cortex from the control group offered valid parameters (Fig. 3: all infections vs. control). When compared with the single *H. bakeri* infection (group H), lactate was found to be increased by *P. berghei* single and *P. berghei-H. bakeri* co-infection (groups P, DC, and SC) in the frontal cortex (Table S1).

In the cerebellum, *P. berghei* infection (groups P and DC) induced a decrease in GPC and IMP compared to uninfected controls. In the brain stem, *P. berghei* as a single infection triggered a large amount of metabolic changes, compared to uninfected controls and *H. bakeri* single infection. Higher relative alanine, valine, and lactate levels were observed in both single and delayed co-infections, whereas GPC was found to be lower in mice infected with *P. berghei* (Fig. 4). In the single infection group, *P. berghei* also caused depleted levels of adenosine, choline, *myo*-inositol, and *N*-acetylaspartate compared to uninfected controls and *H. bakeri* single infection. The spectral profile of the remaining brain tissue was perturbed by both infections. Patent *H. bakeri* infections (groups H and DC) lead to a systematic increase in fumarate, compared to all other groups.

Discussion

The aim of the present work was to characterize the systemic impact of co-infection with two parasitic infections and to determine how a simultaneous or staggered infection with

two parasite species influences host metabolic response. Thus we studied the systemic metabolic perturbations resulting from co-infection with *P. berghei* and *H. bakeri* compared with single infection models and uninfected control mice.

As expected, *P. berghei* generally had a stronger impact on all murine tissues assessed with the exception of the jejunum, than *H. bakeri*, probably explained by the more exacerbated pathology associated with malaria infections.[21] Of the three intestinal regions we examined, only the jejunum was significantly affected by *H. bakeri*. This is consistent with the fact that the nematode resides in the jejunum[22], thus one would expect the parasite to exert its strongest local influence in that intestinal region.

Globally, the simultaneous co-infection model produced the strongest response in spleen and liver metabolism, compared to the other infection models and to the other tissues examined. It appeared to be, however, somewhat protective of dysregulation caused by *P. berghei* and/or *H. bakeri* in the gut and brain, indicated by relatively less metabolic perturbation than each single infection. Although each single infection resulted in a strong statistical model, simultaneous infection of *P. berghei* and *H. bakeri* had the most marked effect on the spleen both in terms of the model strength and the numbers of discriminatory metabolites defining the metabolic phenotype of infection, suggesting that simultaneous impact of the two parasites may cause an enhanced response.

Whilst a delayed co-infection induced an extensive metabolic change in the murine gut, particularly in the ileum, the effects of the simultaneous dual infection were minor and resembled the metabolic profile of *H. bakeri* single infection. Comparing mice with a simultaneous co-infection with uninfected control animals for the brain stem, cerebellum, frontal cortex, and remaining brain regions indicated that there was no significant metabolic difference between these two groups and that the co-infection had no impact on the cerebral metabolism. This was in contrast to *P. berghei* single and delayed co-infection groups, where a range of changes in brain metabolites were observed.

Potential protective effects in co-infection have been the subject of intense research and yet, it is not known what factors are responsible for either protection or increased susceptibility. However, the metabolic discrepancies between delayed and simultaneous co-infection described here, indicate that the timing of a super-infection might be a key factor in disease response to multiple infective agents.

The main metabolic pathways affected by *P. berghei* and *H. bakeri*, either as single or dual infections, were glycolysis, tricarboxylic acid (TCA) cycle, nucleotide, choline, lipid, and amino acid metabolism. We discuss the observed changes pathway by pathway in the next paragraphs.

It has been widely reported that *P. berghei* impacts strongly on glycolysis across numerous tissues and is consistent with the fact that *Plasmodium* relies primarily on glucose and glycolysis for ATP synthesis.[23] Glucose uptake by parasitized red blood cells can increase over 75-fold compared to uninfected cells.[24] Our results are in line with this phenomenon; throughout tissues, groups P (*P. berghei* mono-infection) and DC (delayed co-infection) showed the most pronounced differences regarding glucose and lactate. Hypoglycemia and lactic acidosis are predictors of fatal malaria outcome.[25-27] This predicted decrease of lactate, manifested itself more globally in the *P. berghei* infection groups. In the frontal cortex, brain stem, and remaining brain region, lactate has been found to be increased in groups P and DC, compared to groups H and Ctr. Only in the frontal cortex, group SC displayed an elevated lactate level compared to group H. Unlike lactate, alanine is expressed proportionally to the degree of hypoxia.[28] Alanine was found to be increased in *P. berghei* infection in the brain but also in liver, spleen, and kidney. Surprisingly, increased levels of lactate and alanine were found in the brain stem, although this region is considered hypoxia-resistant.[29]

The effects on the choline metabolism were widespread across biological compartments. Spleen PC and GPC levels were lower in animals with simultaneous co-

infection compared to single infection models and uninfected controls. One explanation may be that choline and its intermediates are recruited for both the generation of new cell membranes to fuel hyperplasia or pro-inflammatory intermediates *via* PC and the arachidonic acid cascade.[30-33]

In the liver, PC was found to be increased in all *P. berghei*-infected mice compared to uninfected controls, whereas choline increased in the *H. bakeri* single infection model compared to uninfected control and group DC. Liver lipid fractions were also found to be higher in groups H and SC compared to controls. The liver is presumably the most important organ for choline metabolism. One of the roles of the liver is to breakdown choline-derivatives to restore choline levels to deprived tissues.[31, 34] Choline can be oxidized into betaine in the kidneys and liver, that can serve as methyl donor for the synthesis of methionine and homocysteine.[35] Betaine was consistently decreased upon *P. berghei* infection in these organs, and further illustrates the extent of the disturbance of the choline metabolism.

In the brain, relative concentrations of choline-related metabolites were generally decreased in *P. berghei* single infection or delayed co-infection. In these infections, choline depletion occurred in the brain stem and remaining brain region, while GPC was decreased in the cerebellum, brain stem, and remaining regions. Depletion of GPC has previously been observed in plasma from *P. berghei*-infected mice.[5, 14] Phosphatidylcholine has been shown to be directly taken up by the intraerythrocytic stage of *P. falciparum*[36], which would affect the normal GPC and choline supply. Decreased GPC levels have been associated with reduced blood flow[37, 38], which supports the idea that sequestration may occur in blood vessels of the brain.

The presence of *H. bakeri* increased choline and GPC levels in the jejunum. It is perhaps not surprising that *H. bakeri* showed a greater impact on the choline metabolism on its close environment reflecting the parasite differences in the balance between systemic and localized effects. Increased levels of choline species may indicate a higher consumption of

choline-containing compounds, such as PC[6, 31] or degradation of biological membranes since GPC is an essential membrane component.[39]

A change in the nucleotide metabolism was observed in every infection model, especially in the central organs and the brain. In the liver and spleen, *P. berghei* infections were illustrated by decreases in inosine and adenosine. In addition, the same trend applied to the pyrimidine derivative uracil, in the spleen. Adenosine is essential in its phosphorylated forms for energy transfer in many metabolic processes[40] and inosine is an intermediate in purine degradation or purine salvage pathways.[41] Uracil is an allosteric regulator and coenzyme in many biological processes such as biosynthesis of polysaccharides and energy metabolism. The degradation of uracil had been suggested in another *P. berghei* murine model.[11] Adenosine levels significantly decreased in the cerebellum, brain stem, and remaining brain tissue in *P. berghei* single infection. Adenosine is a player in many biochemical pathways within the brain, including signaling pathways, nucleic acid metabolism, and homeostasis. With neuroprotective functions, it is involved in preventing brain injury caused by narrowing of vessels caused by stroke.[42] On the contrary, inosine tended to increase in the brain in the presence of *P. berghei* compared to *H. bakeri* single infection or uninfected control animals. Inosine suppresses pro-inflammatory cytokines, particularly IFN-γ, TNF-α, and IL-12.[43, 44] The increased inosine in the brain suggests that it provides a defensive role by preventing injury from congestion of blood vessels by parasitized red blood cells.

Conclusions

To our knowledge, this work represents the first attempt to generate comprehensive data from a range of 10 different tissues in a murine co-infection model. A distinct metabolic phenotype was found for every infection group. The presence of *H. bakeri* displayed only

minimal influence on the gross metabolic effects by *P. berghei*. Overall, *P. berghei* had a strong and systemic impact on the host's energy metabolism with the liver and spleen displaying most pronounced metabolic changes. Infection with *H. bakeri* had a more discrete impact, characterized by fewer but consistent metabolic changes. Most notable changes were observed in the intestine and on the choline/lipid profile.

Comparing the two differently timed dual infections, we have observed that the simultaneous co-infection shows stronger effects on the metabolism of the central organs (liver, spleen, and kidney) when compared to the delayed co-infection, but almost no effects on the metabolism of the gut and brain. The delayed co-infection, however, inflicts significant metabolic disruption at a more systemic level impacting on both central and peripheral organs.

Although the consequences of co-infections are still subject to debate and contradiction, the differences found in the two experimental co-infections indicate that the effects of timing in co-infection warrant further scientific inquiry.

Acknowledgments

We thank Dr. Sergio Wittlin and Jolanda Kamber for support with the *P. berghei* infection. We are grateful to Swiss National Science Foundation (project nos. PPOOA3--114941 and PPOOP3_135170 to J.K.), to the Mathieu-Stiftung (to L.T.) and to the Freiwillige Akademische Gesellschaft Basel (to L.T.) for financial support. Additional support was provided by the Wellcome Trust (grant no. 089002/B/09/Z to J.S.).

References

1. S. Brooker, A. C. Clements, P. J. Hotez, S. I. Hay, A. J. Tatem, D. A. Bundy and R. W. Snow, The co-distribution of *Plasmodium falciparum* and hookworm among African schoolchildren, *Malar J*, 2006, **5**, 99.
2. A. A. Righetti, D. Glinz, L. G. Adiossan, A. Y. Koua, S. Niamke, R. F. Hurrell, R. Wegmuller, E. K. N'Goran and J. Utzinger, Interactions and potential implications of *Plasmodium falciparum*-hookworm coinfection in different age groups in south-central Cote d'Ivoire, *PLoS Negl Trop Dis*, 2012, **6**, e1889.
3. A. A. Adegnika and P. G. Kremsner, Epidemiology of malaria and helminth interaction: a review from 2001 to 2011, *Curr Opin HIV AIDS*, 2012, **7**, 221-224.
4. Y. Wang, S. H. Xiao, J. Xue, B. H. Singer, J. Utzinger and E. Holmes, Systems metabolic effects of a *Necator americanus* infection in Syrian hamster, *J Proteome Res*, 2009, **8**, 5442-5450.
5. J. V. Li, Y. Wang, J. Saric, J. K. Nicholson, S. Dirnhofer, B. H. Singer, M. Tanner, S. Wittlin, E. Holmes and J. Utzinger, Global metabolic responses of NMRI mice to an experimental *Plasmodium berghei* infection, *J Proteome Res*, 2008, **7**, 3948-3956.
6. J. Saric, J. V. Li, J. Utzinger, Y. Wang, J. Keiser, S. Dirnhofer, O. Beckonert, M. T. Sharabiani, J. M. Fonville, J. K. Nicholson and E. Holmes, Systems parasitology: effects of *Fasciola hepatica* on the neurochemical profile in the rat brain, *Mol Syst Biol*, 2010, **6**, 396.
7. Y. Wang, J. V. Li, J. Saric, J. Keiser, J. Wu, J. Utzinger and E. Holmes, Advances in metabolic profiling of experimental nematode and trematode infections, *Adv Parasitol*, 2010, **73**, 373-404.
8. Y. Wang, E. Holmes, J. K. Nicholson, O. Cloarec, J. Chollet, M. Tanner, B. H. Singer and J. Utzinger, Metabonomic investigations in mice infected with *Schistosoma mansoni*: an approach for biomarker identification, *Proc Natl Acad Sci U S A*, 2004, **101**, 12676-12681.

9. J. Saric, J. V. Li, Y. Wang, J. Keiser, K. Veselkov, S. Dirnhofer, I. K. Yap, J. K. Nicholson, E. Holmes and J. Utzinger, Panorganismal metabolic response modeling of an experimental *Echinostoma caproni* infection in the mouse, *J Proteome Res*, 2009, **8**, 3899-3911.

10. S. Ghosh, A. Sengupta, S. Sharma and H. M. Sonawat, Metabolic fingerprints of serum, brain, and liver are distinct for mice with cerebral and noncerebral malaria: a $^{(1)}$H NMR spectroscopy-based metabonomic study, *J Proteome Res*, 2012, **11**, 4992-5004.

11. A. Basant, M. Rege, S. Sharma and H. M. Sonawat, Alterations in urine, serum and brain metabolomic profiles exhibit sexual dimorphism during malaria disease progression, *Malar J*, 2010, **9**, 110.

12. A. Sengupta, A. Basant, S. Ghosh, S. Sharma and H. M. Sonawat, Liver Metabolic Alterations and Changes in Host Intercompartmental Metabolic Correlation during Progression of Malaria, *J Parasitol Res*, 2011, **2011**, 901854.

13. J. Behnke and P. D. Harris, *Heligmosomoides bakeri*: a new name for an old worm?, *Trends Parasitol*, 2010, **26**, 524-529.

14. L. Tritten, J. Keiser, M. Godejohann, J. Utzinger, M. Vargas, O. Beckonert, E. Holmes and J. Saric, Metabolic profiling framework for discovery of candidate diagnostic markers of malaria, *Sci Rep*, 2013, **3**, 2769.

15. U. Nwosu, M. Vargas, A. Harder and J. Keiser, Efficacy of the cyclooctadepsipeptide PF1022A against *Heligmosomoides bakeri in vitro* and *in vivo*, *Parasitology*, 2011, 1-9.

16. B. Franke-Fayard, H. Trueman, J. Ramesar, J. Mendoza, M. van der Keur, R. van der Linden, R. E. Sinden, A. P. Waters and C. J. Janse, A *Plasmodium berghei* reference line that constitutively expresses GFP at a high level throughout the complete life cycle, *Mol Biochem Parasitol*, 2004, **137**, 23-33.

17. J. K. Nicholson, P. J. Foxall, M. Spraul, R. D. Farrant and J. C. Lindon, 750 MHz ^{1}H and ^{1}H-^{13}C NMR spectroscopy of human blood plasma, *Anal Chem*, 1995, **67**, 793-811.

18. K. A. Veselkov, L. K. Vingara, P. Masson, S. L. Robinette, E. Want, J. V. Li, R. H. Barton, C. Boursier-Neyret, B. Walther, T. M. Ebbels, I. Pelczer, E. Holmes, J. C. Lindon and J. K. Nicholson, Optimized preprocessing of ultra-performance liquid chromatography/mass spectrometry urinary metabolic profiles for improved information recovery, *Anal Chem*, 2011, **83**, 5864-5872.

19. J. Trygg and S. Wold, Orthogonal projections to latent structures (O-PLS), *Journal of Chemometrix*, 2002, **16**, 119-128.

20. O. Cloarec, M. E. Dumas, J. Trygg, A. Craig, R. H. Barton, J. C. Lindon, J. K. Nicholson and E. Holmes, Evaluation of the orthogonal projection on latent structure model limitations caused by chemical shift variability and improved visualization of biomarker changes in ^{1}H NMR spectroscopic metabonomic studies, *Anal Chem*, 2005, **77**, 517-526.

21. A. Trampuz, M. Jereb, I. Muzlovic and R. M. Prabhu, Clinical review: Severe malaria, *Crit Care*, 2003, **7**, 315-323.

22. J. M. Behnke, D. M. Menge and H. Noyes, *Heligmosomoides bakeri*: a model for exploring the biology and genetics of resistance to chronic gastrointestinal nematode infections, *Parasitology*, 2009, **136**, 1565-1580.

23. J. I. MacRae, M. W. Dixon, M. K. Dearnley, H. H. Chua, J. M. Chambers, S. Kenny, I. Bottova, L. Tilley and M. J. McConville, Mitochondrial metabolism of sexual and asexual blood stages of the malaria parasite *Plasmodium falciparum*, *BMC Biol*, 2013, **11**, 67.

24. I. W. Sherman, Biochemistry of *Plasmodium* (malarial parasites), *Microbiol Rev*, 1979, **43**, 453-495.

25. F. C. Howarth, A. Qureshi and J. Singh, Effects of acidosis on ventricular myocyte shortening and intracellular Ca^{2+} in streptozotocin-induced diabetic rats, *Mol Cell Biochem*, 2004, **261**, 227-233.

26. S. Ehrhardt, F. P. Mockenhaupt, S. D. Anemana, R. N. Otchwemah, D. Wichmann, J. P. Cramer, U. Bienzle, G. D. Burchard and N. W. Brattig, High levels of circulating cardiac proteins indicate cardiac impairment in African children with severe *Plasmodium falciparum* malaria, *Microbes Infect*, 2005, **7**, 1204-1210.

27. R. T. Robinson, N. D. Harris, R. H. Ireland, S. Lee, C. Newman and S. R. Heller, Mechanisms of abnormal cardiac repolarization during insulin-induced hypoglycemia, *Diabetes*, 2003, **52**, 1469-1474.

28. O. Ben-Yoseph, R. S. Badar-Goffer, P. G. Morris and H. S. Bachelard, Glycerol 3-phosphate and lactate as indicators of the cerebral cytoplasmic redox state in severe and mild hypoxia respectively: a ^{13}C- and ^{31}P-n.m.r. study, *Biochem J*, 1993, **291 (Pt 3)**, 915-919.

29. T. M. Tsang, J. L. Griffin, J. Haselden, C. Fish and E. Holmes, Metabolic characterization of distinct neuroanatomical regions in rats by magic angle spinning ^{1}H nuclear magnetic resonance spectroscopy, *Magn Reson Med*, 2005, **53**, 1018-1024.

30. P. C. Calder, Polyunsaturated fatty acids and inflammatory processes: New twists in an old tale, *Biochimie*, 2009, **91**, 791-795.

31. Z. Li and D. E. Vance, Phosphatidylcholine and choline homeostasis, *J Lipid Res*, 2008, **49**, 1187-1194.

32. J. Saric, Interactions between immunity and metabolism - contributions from the metabolic profiling of parasite-rodent models, *Parasitology*, 2010, **137**, 1451-1466.

33. S. H. Zeisel and K. A. da Costa, Choline: an essential nutrient for public health, *Nutr Rev*, 2009, **67**, 615-623.

34. Z. Li, L. B. Agellon and D. E. Vance, Phosphatidylcholine homeostasis and liver failure, *J Biol Chem*, 2005, **280**, 37798-37802.

35. D. D. Tyler, Transport and oxidation of choline by liver mitochondria, *Biochem J*, 1977, **166**, 571-581.

36. A. P. Simoes, G. N. Moll, A. J. Slotboom, B. Roelofsen and J. A. Op den Kamp, Selective internalization of choline-phospholipids in *Plasmodium falciparum* parasitized human erythrocytes, *Biochim Biophys Acta*, 1991, **1063**, 45-50.

37. J. Kuhmonen, J. Sivenius, P. J. Riekkinen, Sr. and R. A. Kauppinen, Decrease in brain choline-containing compounds following a short period of global ischemia in gerbils as detected by ^{1}H NMR spectroscopy *in vivo*, *NMR Biomed*, 1994, **7**, 231-236.

38. M. Wilson, N. P. Davies, M. A. Brundler, C. McConville, R. G. Grundy and A. C. Peet, High resolution magic angle spinning ^{1}H NMR of childhood brain and nervous system tumours, *Mol Cancer*, 2009, **8**, 6.

39. J. Klein, Membrane breakdown in acute and chronic neurodegeneration: focus on choline-containing phospholipids, *J Neural Transm*, 2000, **107**, 1027-1063.

40. B. Schoepp-Cothenet, R. van Lis, A. Atteia, F. Baymann, L. Capowiez, A. L. Ducluzeau, S. Duval, F. ten Brink, M. J. Russell and W. Nitschke, On the universal core of bioenergetics, *Biochim Biophys Acta*, 2013, **1827**, 79-93.

41. A. W. Murray, The biological significance of purine salvage, *Annu Rev Biochem*, 1971, **40**, 811-826.

42. H. Y. Shen, T. A. Lusardi, R. L. Williams-Karnesky, J. Q. Lan, D. J. Poulsen and D. Boison, Adenosine kinase determines the degree of brain injury after ischemic stroke in mice, *J Cereb Blood Flow Metab*, 2011, **31**, 1648-1659.

43. J. G. Mabley, A. Rabinovitch, W. Suarez-Pinzon, G. Hasko, P. Pacher, R. Power, G. Southan, A. Salzman and C. Szabo, Inosine protects against the development of diabetes in multiple-low-dose streptozotocin and nonobese diabetic mouse models of type 1 diabetes, *Mol Med*, 2003, **9**, 96-104.

44. G. Hasko, M. V. Sitkovsky and C. Szabo, Immunomodulatory and neuroprotective effects of inosine, *Trends Pharmacol Sci*, 2004, **25**, 152-157.

539

Figures and Figure Legends

Fig. 1

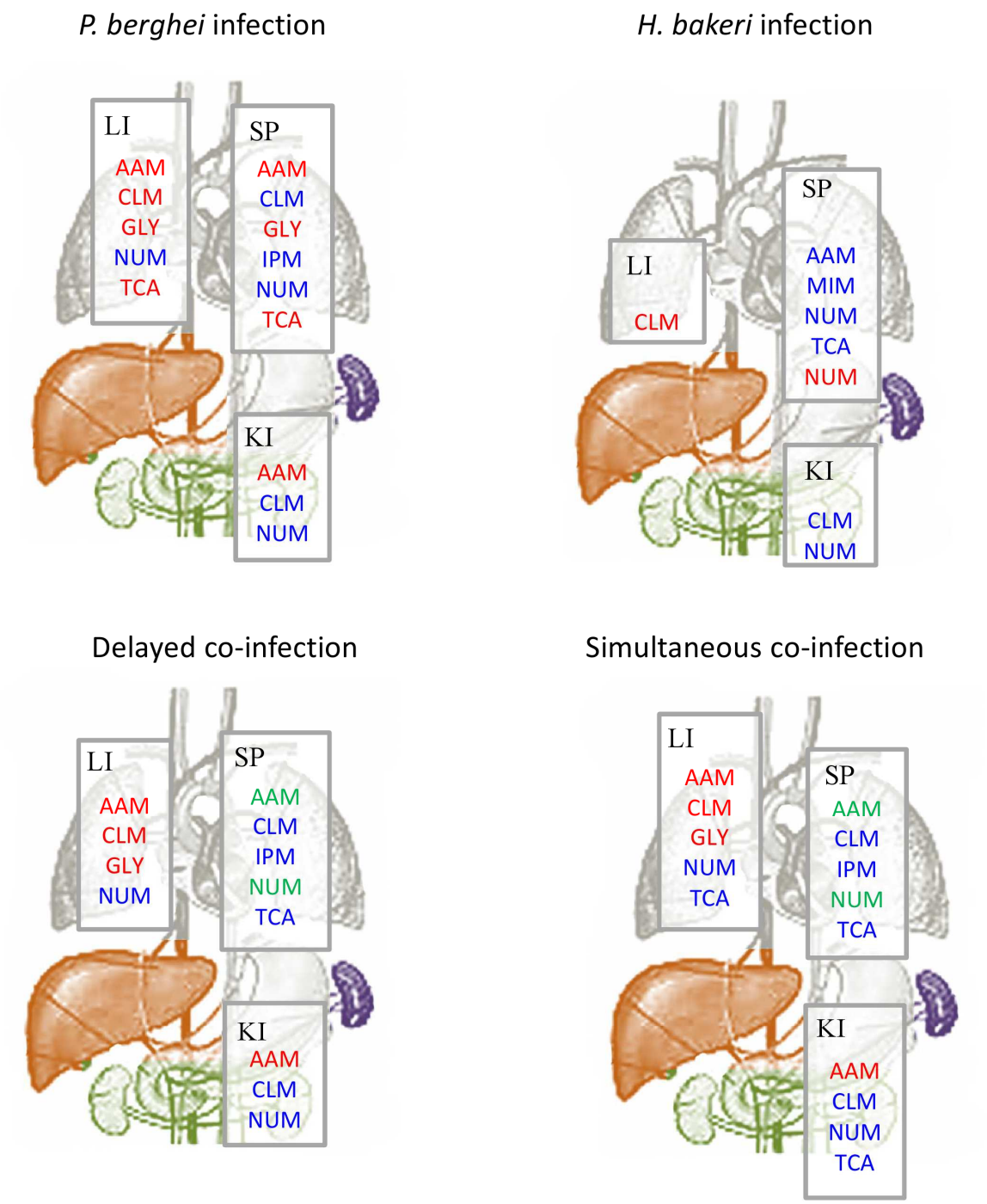

Fig. 1 Metabolic biomarkers recovered in central organs. Metabolic compartments affected in central organs upon *P. berghei* or *H. bakeri* single infection, and in two co-infection models. Key: LI: liver; SP: spleen; KI: kidney. **Red**, relatively increased in infected animals when

546 compared to the uninfected control group; **Blue**, relative lower levels in the respective
547 infection group when compared to the uninfected control group; **Green**, some metabolites
548 are increased and others decreased due to infection; AAM, amino acid metabolism; CLM,
549 choline and lipid metabolism; FAM, fatty acid metabolism; GLY, glycolysis; IMP, inositol
550 phosphate metabolism; NUM, nucleotide metabolism; TCA, tricarboxylic acid cycle.
551
552

553 **Fig. 2**

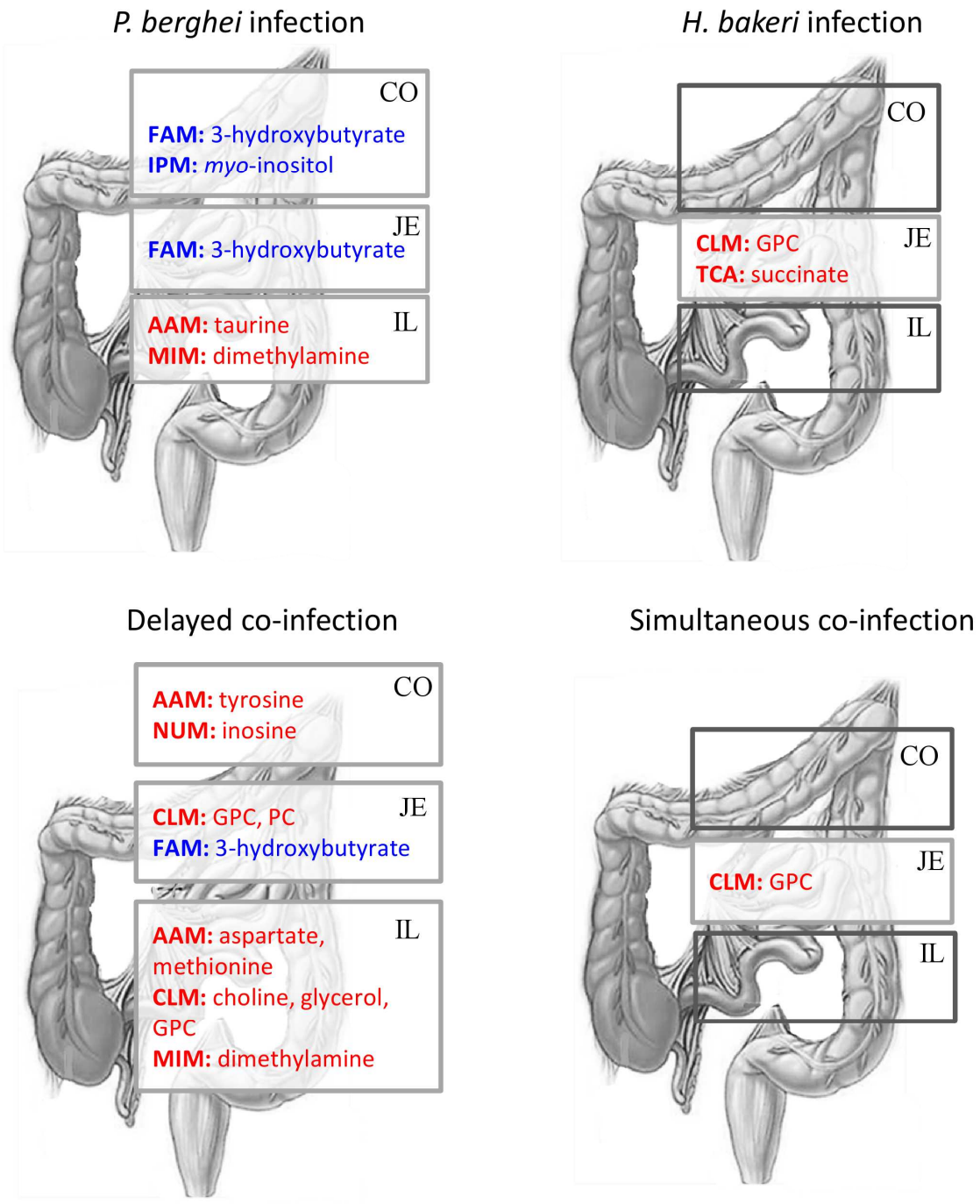

554

555

556 **Fig. 2** Metabolic biomarkers recovered from three different sections of the gut. Key
557 metabolite changes in murine intestinal tissue upon *P. berghei* or *H. bakeri* single infection,
558 and in two co-infection models. Key: CO: colon; IL: ileum; JE: jejunum. **Red,** relatively
559 increased in infected animals when compared to the uninfected control group; **Blue**, relative

560 lower levels in the respective infection group when compared to the uninfected control group;
561 AAM, amino acid metabolism; CLM, choline and lipid metabolism; FAM, fatty acid
562 metabolism; MIM, microbial metabolism; NUM, nucleotide metabolism.
563
564 **Fig. 3**

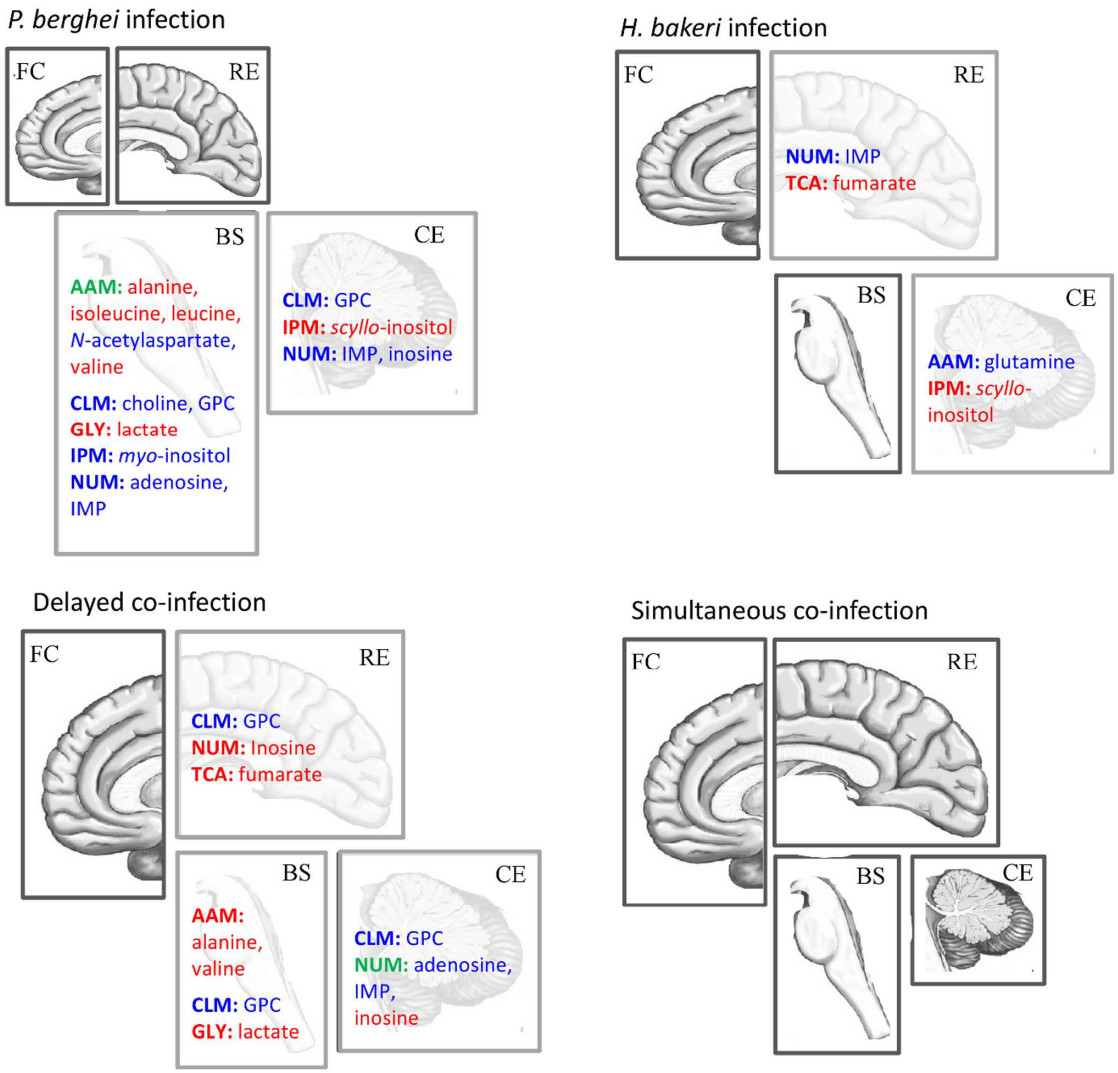

565
566 **Fig. 3** Biomarkers identified across four different brain sections. Main metabolite changes
567 occurring in neural tissue from mice differentially infected with *P. berghei* or *H. bakeri*, or in
568 two co-infection models. Key: BS: brain stem; CE: cerebellum; FC: frontal cortex; RT:
569 remaining tissue. **Red:** relatively increased in infected animals when compared to the control
570 group; **Blue:** relative lower levels in the respective infection group when compared to the

control group; **Green:** some metabolites are increased and others decreased due to infection; AAM, amino acid metabolism; CLM, choline and lipid metabolism; GLY, glycolysis; GPC, glycerophosphocholine; IMP, inosine monophosphate; IPM, inositol phosphate metabolism; NUM, nucleotide metabolism; TCA, tricarboxylic acid cycle.

Fig. 4

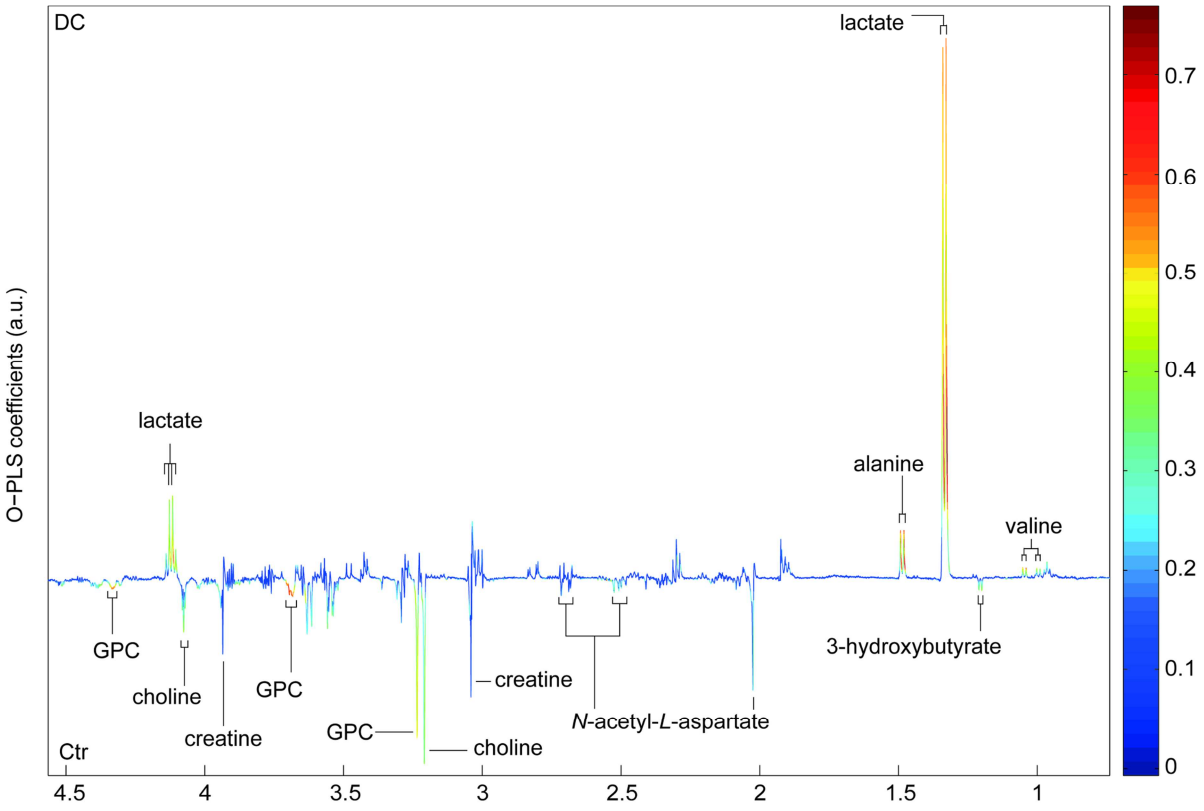

Fig. 4 ^{1}H NMR-derived brain stem spectrum in delayed co-infection. O-PLS-DA coefficient plot of ^{1}H NMR data obtained from brain stem extracts in delayed co-infection compared to the uninfected control group. Key: a.u., arbitrary units; Ctr, control group; DC, delayed co-infection; GPC, glycerophosphocholine. Red represents high significance and blue represents low significance.